



Article

Assessment and Data Fusion of Satellite-Based Precipitation Estimation Products over Ungauged Areas Based on Triple Collocation without In Situ Observations

Xiaoqing Wu^{1,2}, Jialiang Zhu² and Chengguang Lai^{1,3,*}

¹ School of Civil Engineering and Transportation, South China University of Technology, Guangzhou 510641, China; wuxiaoqing@scies.org

² The Key Laboratory of Water and Air Pollution Control of Guangdong Province, South China Institute of Environmental Sciences, Ministry of Ecology and Environment of the People's Republic of China, Guangzhou 510535, China; zhujialiang@scies.org

³ Pazhou Lab, Guangzhou 510335, China

* Correspondence: laichg@scut.edu.cn

Abstract: Reliable assessment of satellite-based precipitation estimation (SPE) and production of more accurate precipitation data by data fusion is typically challenging in sparsely gauged and ungauged areas. Triple collocation (TC) is a novel assessment approach that does not require gauge observations; it provides a feasible solution for this problem. This study comprehensively validates the TC performance for assessing SPEs and performs data fusion of multiple SPEs using the TC-based merging (TCM) approach. The study area is the Tibetan Plateau (TP), a typical area lacking gauge observations. Three widely used SPEs are used: the integrated multi-satellite retrievals for global precipitation measurement (IMERG) “early run” product (IMERG-E), the precipitation estimation from remotely sensed information using artificial neural networks (PERSIANN) dynamic infrared (PDIR), and the Climate Prediction Center (CPC) morphing technique (CMORPH). Validation of the TC assessment approach shows that TC can effectively assess the SPEs’ accuracy, derive the spatial accuracy pattern of the SPEs, and reveal the accuracy ranking of the SPEs. TC can also detect the SPEs’ accuracy patterns, which are difficult to obtain from a traditional approach. The data fusion results of the SPEs show that TCM incorporates the regional advantages of the individual SPEs, providing more accurate precipitation data than the original SPEs, revealing that data fusion is reasonable and reliable in ungauged areas. In general, the TC approach performs well for the assessment and data fusion of SPEs, showing reasonable applicability in the TP and other areas lacking gauge data than other methods because it does not rely on gauge observations.

Keywords: triple collocation; satellite-based precipitation estimation (SPE); accuracy assessment; data fusion; ungauged areas; Tibetan Plateau



Citation: Wu, X.; Zhu, J.; Lai, C. Assessment and Data Fusion of Satellite-Based Precipitation Estimation Products over Ungauged Areas Based on Triple Collocation without In Situ Observations. *Remote Sens.* **2023**, *15*, 4210. <https://doi.org/10.3390/rs15174210>

Academic Editor: Luca Brocca

Received: 9 June 2023

Revised: 23 August 2023

Accepted: 25 August 2023

Published: 27 August 2023



Copyright: © 2023 by the authors. Licensee MDPI, Basel, Switzerland. This article is an open access article distributed under the terms and conditions of the Creative Commons Attribution (CC BY) license (<https://creativecommons.org/licenses/by/4.0/>).

1. Introduction

Reliable precipitation data are essential for meteorological, agricultural, water resource, and hydrological applications [1–5]. Ground observations from gauge stations are typically used to obtain accurate precipitation data. Nevertheless, due to rugged terrain and hostile environments, ground-based gauge stations are difficult to establish and maintain in many areas worldwide, resulting in a sparse and uneven distribution of local gauge observations and limiting the spatial representativeness and reliability of precipitation data [4,6,7].

Several satellite-based precipitation estimation (SPE) products were developed and released in the last decade, providing wide coverage, spatiotemporal continuity, and high-resolution precipitation data based on satellite remote sensing information. These products have substantial potential as an alternative precipitation data source for the Tibetan Plateau (TP) and other ungauged areas [2]. Widely used SPEs include the precipitation estimation

from remotely sensed information using artificial neural networks (PERSIANN) series [8], which is predominantly based on infrared (IR) data, the Climate Prediction Center (CPC) morphing technique (CMORPH) series [9], which uses passive microwave (PMW) data, the tropical rainfall measuring mission (TRMM) multi-satellite precipitation analysis (TMPA) products [10], and the successor of the TMPA, i.e., the integrated multi-satellite retrievals for global precipitation measurement (IMERG) series [11,12], which integrates IR, PMW, and spaceborne radar data. These SPEs are produced by different retrieval algorithms and have been widely used in several studies on the TP. Nevertheless, due to interference with remote sensing signals and retrieval algorithms' limitations, SPEs usually have nonnegligible errors [7,13,14]. The error characteristics depend on the type of SPE product, area, season, regional conditions, satellite data sources, and retrieval algorithms [4,13]. Therefore, it is typically necessary to assess the accuracy and error features of the SPEs before use and improve the SPE accuracy if needed. Merging multiple SPEs using data fusion is widely regarded as an effective strategy to improve the precipitation data products because the relative advantages of different data sources are incorporated [4,13,15,16].

Many studies have assessed the accuracy and error characteristics of SPEs [7,17–24] and merged multiple SPEs to improve the quantitative precipitation estimates [3,4,25,26]. Related studies have been performed in many areas worldwide, including the TP. Nevertheless, most previous studies that assessed SPEs used ground-based gauge data, which are regarded as the “true value” of precipitation and are used as the assessment benchmark. Multi-SPE data fusion also relies on the quantitative accuracy assessment results of the SPEs based on gauge data. Therefore, challenges remain in the assessment and data fusion of SPEs in areas with limited gauge data, such as the TP. Recently, the triple collocation (TC) approach [27,28] was proposed as a novel strategy to assess estimates of geophysical variables without the need for benchmark data. This method provides a solution for assessing SPEs and performing data fusion in ungauged areas. The TC approach was developed to assess ocean wind speed products, but it was also successfully used to assess many other geophysical variables, including soil moisture [29], soil freezing/thawing [30], and water storage [31]. Unlike the traditional approach that relies on benchmark data, the TC approach indirectly derives the error and accuracy of the estimations by evaluating the statistical relationships between different independent data sources [27,32,33]. Therefore, the TC approach requires three estimations as input (called the triplet), which should be mutually independent data sources or estimation mechanisms. Specifically, the TC approach assumes that the estimation inputs have zero error cross-correlation (ECC).

Recently, the TC approach was used to assess SPEs and other precipitation estimation products globally and regionally in central and west Asia, the continental U.S., and mainland China [33–37]. Furthermore, Tang et al. [2] used the TC approach to assess the accuracy of SPEs for snowfall estimation. Bai et al. [38] evaluated the drought performance of long-term SPEs with the TC approach. Reanalysis data, such as that retrieved from satellite soil moisture estimations by the fifth generation of European ReAnalysis (ERA5) and the SM2RAIN SPE product, have been widely used as the triplet in the TC approach because their widely differing mechanisms meet the TC requirements [38,39]. These studies have demonstrated the ability of the TC approach to quantify the error of SPEs, indicating the potential of SPE data fusion based on the SPE error characteristics derived by the TC approach for areas with limited gauge observations. Yilmaz et al. [40] proposed a least-squares-based data fusion framework utilizing the outputs of the TC approach. Based on this framework, Dong et al. [41] and Lyu et al. [42] performed data fusion for SPEs and reanalysis data and found that the merged precipitation product outperformed the individual input data. Chen et al. [13] found that the TC-based merging (TCM) approach showed comparable performance to the gauge-based Bayesian model averaging approach. Nevertheless, these studies used the triplet members of the TC assessment approach, including reanalysis and SM2RAIN data, as precipitation data input for data fusion. This strategy might cause difficulty producing long-term or near-real-time merged data products because the SM2RAIN

is not an hourly-scale near-real-time product. Few studies considered TC-based data fusion of precipitation products not limited to the triplet members of the TC approach.

The goal of this study is to evaluate TC-based accuracy assessment and data fusion of SPEs in ungauged areas. This study focuses on the use of TC-based precipitation data assessment and fusion in the TP, an area which receives wide attention and is called “the Asian water tower” but which suffers from scarcity of in situ gauge observations due to the high mountain and plateau terrain. The objectives of this study are (1) to investigate the performance of the TC approach in assessing the accuracy of several SPEs in the TP and (2) evaluate the data fusion performance of the SPEs based on their error characteristics derived by the TC approach without gauge observations. Three widely used SPEs are used for data fusion: IMERG, PERSIANN-Dynamic Infrared (PDIR), and CMORPH. Different to previous studies on TC-based data fusion, this study (1) focuses on TC-based data fusion for the TP, an area playing a vital role in freshwater supply and as a climate indicator for Asia [1] but less considered in former related studies, and (2) uses the satellite-only SPE products as fusion inputs to ensure the timeliness and adequate data record length of the merged products, while reanalysis and SM2RAIN are only utilized to assist to derive the error of the SPE by the TC approach. This study provides new insights into improving precipitation estimations in the TP and other sparsely gauged/ungauged areas.

2. Study Area and Data

2.1. Tibetan Plateau

The TP is located in southwestern China in central Asia (70° to 105° longitude and 25° to 40° latitude) and has an area of about 2.5 million km² (Figure 1). The TP has the highest mean altitude above sea level (over 4000 m) worldwide and is known as the “roof of the world” and the “Earth’s third pole”. Due to the high elevation and complex topography, the TP has a cold and arid plateau and alpine climate, with annual mean precipitation ranging from more than 1000 mm in the southeast to close to zero in the northwest. The mean air temperature ranges from −6 °C to 2.6 °C. As a result, the TP has a unique landscape consisting of alpine grasslands, deserts, and glaciers, with fragile ecosystems. The TP is also the headwater region of several major rivers in Asia, including the Yellow, Yangtze, Mekong, Salween, Brahmaputra, Ganges, and Indus rivers; thus, the TP is also called the “Asia water tower”. Due to climate change, the air temperature has increased and is increasing in the TP, significantly altering the local hydrological cycle and affecting the global climate system [1,4,7,43]. Reliable precipitation data for the TP are not only essential for local water resource management and environmental and ecological applications but also for understanding how the energy balance of the TP influences global climate change [4,30,43–46]. Nevertheless, gauge observations are sparse in the TP and non-existent in the northwestern part, indicating the urgent requirement for substitute precipitation datasets.

2.2. Gauge Observations

Daily precipitation observation data from 2007 to 2018 were obtained from 177 gauge stations in and around the TP (see Figure 1). The gauge data were downloaded from the data service website of the China Meteorological Administration (CMA) (data.cma.cn, accessed on 25 May 2023). The gauge data have undergone rigorous quality control procedures, including checking extreme values, internal consistency, and spatial consistency, and assigning quality control codes to ensure data reliability [4,7]. The gauge data records that did not have a “correct” code (less than 3%) were not used in the assessment. The gauge precipitation data were not used for SPE data fusion but only as a benchmark to validate the performance of the TC approach for assessing SPEs and the accuracy of the multi-SPE merged products.

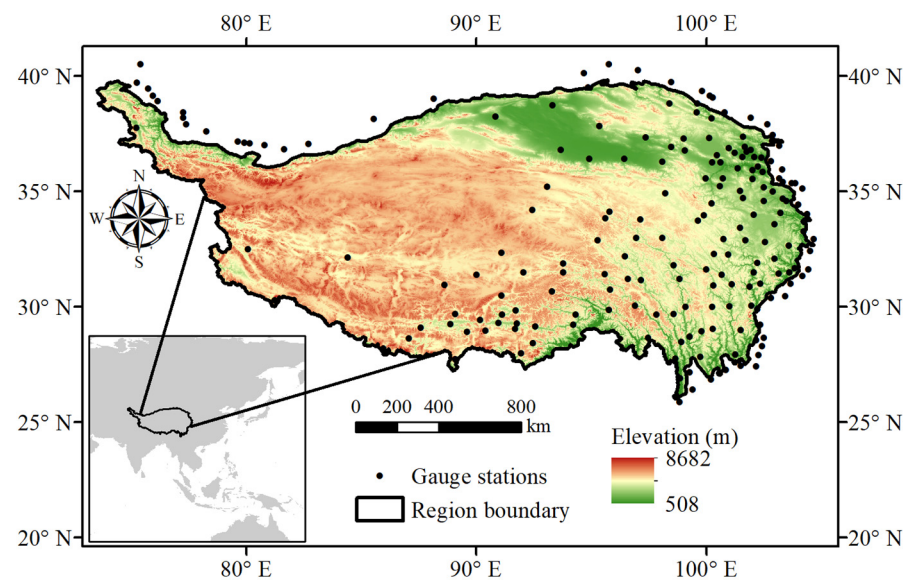


Figure 1. Geographical location of the TP and the gauge stations.

2.3. Satellite-Based Precipitation Estimation Products

1. IMERG

The IMERG product series provided by the Global Precipitation Mission (GPM) [11] is a state-of-the-art and widely used global SPE product. It aims to intercalibrate, merge, and interpolate most satellite precipitation estimates to provide wide-coverage and high-spatiotemporal resolution precipitation data. The latest version, v6, of the IMERG product provides long-term precipitation records (since June 2000) with a spatial resolution of 0.1° , integrating IR, PMW, and spaceborne radar data from several satellite meteorology and precipitation monitoring missions using the Goddard profiling (GPROF) algorithm [11]. The IMERG product series consists of two near-real-time precipitation products (“early run” and “late run”) solely produced from satellite data and one post-processing product (“final run”) merged with ground-based gauge observations timestep-by-timestep. Since the gauge observation data used in this study might include gauge data already merged with the IMERG products, we used only the near-real-time “early run” IMERG product (hereafter referred to as IMERG-E), which did not undergo gauge correction. The data of the IMERG product were downloaded from the GPM website (<https://gpm.nasa.gov/data/directory>, accessed on 25 May 2023).

2. PDIR

The PDIR [47] is a state-of-the-art SPE product of the PERSIANN series developed by the Center for Hydrometeorology and Remote Sensing (CHRS) at the University of California, Irvine (UCI). It provides short-latency (below one hour), real-time, high-resolution (0.04°) precipitation data for real-time hydrological applications, such as flood predictions and flood maps. The PDIR data have broad spatial coverage (60°S – 60°N) and a relatively long data record (since 2000). The PDIR was chosen from the PERSIANN products because it is solely based on satellite data, not gauge data. The PDIR product is based on high-frequency IR imagery that is processed by an improved cloud segmentation algorithm and dynamically adopted by different cloud top temperature–rain rate (Tb-R) curves according to the classified cloud patches to generate precipitation estimations [48]. The daily PDIR data were downloaded from the data portal website of the CHRS (<http://chrsdata.eng.uci.edu/>, accessed on 25 May 2023).

3. CMORPH

CMORPH [9] is a widely used and widely validated SPE developed by the National Oceanic and Atmospheric Administration (NOAA) Climate Prediction Center (CPC). It

consists of precipitation data since 1998 with a spatial coverage of 60°S–60°N and a resolution of 0.25°. Unlike IMERG and PDIR, CMORPH is produced by a morphing algorithm that uses geostationary satellite IR data to derive the cloud motion field. We used the CMORPH bias-corrected product (CMORPH-CRT), a satellite-based product produced by probability distribution function matching and corrected by gauge observations. Note that the CMORPH-CRT was only processed by the climatological bias-correction to eliminate the seasonal systematic bias, but not directly merged with the gauge observations (the gauge-blended version name is CMORPH-BLD). Therefore, the CMORPH-CRT can, thus, be regarded as similar to satellite-only SPE. The daily CMORPH data were downloaded from the CPC website (https://ftp.cpc.ncep.noaa.gov/precip/CMORPH_V1.0/, accessed on 25 May 2023).

2.4. Other Gridded Precipitation Products

1. ERA5

The ERA5 [49] is a model-based reanalysis data product with a different production mechanism to the SPEs. It was utilized as the triplet input to the TC approach with the SPE to meet the TC requirement of three independent data inputs. ERA5 is a state-of-the-art global reanalysis data product developed by the European Center for Medium-range Weather Forecasts (ECMWF), providing reanalysis data of several atmospheric variables, including precipitation at 0.25° resolution. The ERA5 data were produced by a numerical weather forecast model called the integrated forecasting system (IFS Cycle 41r2) and a four-dimensional variational data assimilation algorithm. The daily ERA5 precipitation data were downloaded from the Copernicus Climate Change Service (C3S) website (<https://doi.org/10.24381/cds.f17050d7>, accessed on 25 May 2023).

2. SM2RAIN-ASCAT

The SM2RAIN-Advanced SCATterometer (ASCAT) product [49] also has a production mechanism distinct from conventional SPEs. It was used as another data product to constitute the TC triplet together with the SPEs. Unlike conventional SPEs with a top-down monitoring scheme, the SM2RAIN-ASCAT data are inversion products derived from soil moisture data retrieved by satellite remote sensing and a water balance model [50,51]. The soil moisture data for producing the SM2RAIN-ASCAT are acquired by the ASCAT onboard the MetOp satellite and have not been used by other SPEs. Therefore, the SM2RAIN-ASCAT has different retrieval mechanisms to conventional SPEs and represents an independent data source; thus, it has been widely used as part of the triplet with other SPEs in the TC approach. SM2RAIN-ASCAT provides daily precipitation data from 2007 and onwards with a spatial resolution of 12.5 km.

3. Methods

3.1. The Triple Collocation (TC) Approach

The TC approach [27,28] derives the error and accuracy of precipitation estimations without benchmark data. It requires three estimations as inputs, called the triplet, and is based on the assumption that the inputs are independent data sources or have independent mechanisms. More specifically, the error of the estimates of the triplet should be uncorrelated, i.e., the ECC should be zero. The TC approach is based on an additive error model as follows:

$$P_i = \alpha_i + \beta_i T + \varepsilon_i \quad (1)$$

where P_i is the estimate of one of the triplet members (ERA5, SM2RAIN-ASCAT, and an SPE in this study); when i is 1, 2, or 3, it indicates one of the three triplet members, respectively; T is the unknown true value; α_i and β_i are the linear regression coefficients representing the systematic error; ε_i is the random error.

The covariance between any two estimations of the triplet (denoted as C_{ij}) can be expressed as:

$$C_{ij} = \beta_i \beta_j \sigma^2(T) + \beta_j \text{Cov}(\varepsilon_i, T) + \beta_i \text{Cov}(\varepsilon_j, T) + \alpha_j E(\varepsilon_i) + \alpha_i E(\varepsilon_j) + \text{Cov}(\varepsilon_i, \varepsilon_j) \quad (2)$$

where $\sigma^2(\cdot)$ and $E(\cdot)$ denote the variance and expected value, respectively. According to the assumptions of the TC approach, the random errors ε_i should be zero, i.e., $E(\varepsilon_i) = 0$; the ε_i are uncorrelated with the true values, i.e., $\text{Cov}(\varepsilon_i, T) = 0$. The ECC should be zero, i.e., $\text{Cov}(\varepsilon_i, \varepsilon_j) = 0$ when $i \neq j$. Thus, the C_{ij} can be expressed as:

$$\begin{cases} C_{ij} = \beta_i \beta_j \sigma^2(T) \\ C_{ii} = \beta_i^2 \sigma^2(T) + \sigma^2(\varepsilon_i) \end{cases} \quad (3)$$

By solving Equation (3), the error variance $\sigma^2(\varepsilon_i)$ of the three triplet members, which can be used to quantify the error of the estimate, can be derived as:

$$\begin{cases} \sigma^2(\varepsilon_1) = C_{11} - \frac{C_{12}C_{13}}{C_{23}} \\ \sigma^2(\varepsilon_2) = C_{22} - \frac{C_{12}C_{23}}{C_{13}} \\ \sigma^2(\varepsilon_3) = C_{33} - \frac{C_{13}C_{23}}{C_{12}} \end{cases} \quad (4)$$

McColl et al. [27] improved the TC approach by calculating the correlation coefficient (CC) between the estimate and the unknown true values to quantify the accuracy of the estimates. According to Equation (1), the CC of the i th triplet member can be derived as:

$$CC_i = \frac{\text{Cov}(P_i, T)}{\sqrt{\sigma^2(P_i)} \cdot \sqrt{\sigma^2(T)}} = \frac{\beta_i \sigma^2(T)}{\sqrt{\sigma^2(P_i)} \cdot \sqrt{\sigma^2(T)}} = \frac{\beta_i \sqrt{\sigma^2(T)}}{\sqrt{C_{ii}}} \quad (5)$$

By solving Equations (3) and (5), the CCs of the triplet members can be derived as:

$$\begin{cases} CC_1 = \sqrt{\frac{C_{12}C_{13}}{C_{23}C_{11}}} \\ CC_2 = \sqrt{\frac{C_{12}C_{23}}{C_{13}C_{22}}} \\ CC_3 = \sqrt{\frac{C_{13}C_{23}}{C_{12}C_{33}}} \end{cases} \quad (6)$$

3.2. TC-Based Merging Approach

Yilmaz et al. [40] proposed a data fusion approach based on the error derived from the TC approach and the least-squares theory, which is called the TCM approach in this study. Data fusion is achieved by the weighted averaging of the data input:

$$P_{TCM} = w_1 P_1 + w_2 P_2 + \dots + w_k P_k + \dots + w_n P_n \quad (7)$$

where P_{TCM} is the merged SPE; P_k is the k th SPE to be merged; n is the total number of SPEs; w_k is the weight of the k th SPE inferred from the TC-derived error ($w_1 + w_2 + \dots + w_n = 1$). By minimizing the error variance of P_{TCM} , the weights in Equation (7) can be derived as

the functions of the error variance of the SPEs [13,40]. The weights of the three SPEs can be derived as:

$$\begin{cases} w_1 = \frac{\sigma^2(\varepsilon_2)\sigma^2(\varepsilon_3)}{\sigma^2(\varepsilon_1)\sigma^2(\varepsilon_2) + \sigma^2(\varepsilon_2)\sigma^2(\varepsilon_3) + \sigma^2(\varepsilon_1)\sigma^2(\varepsilon_3)} \\ w_2 = \frac{\sigma^2(\varepsilon_1)\sigma^2(\varepsilon_2)}{\sigma^2(\varepsilon_1)\sigma^2(\varepsilon_2) + \sigma^2(\varepsilon_2)\sigma^2(\varepsilon_3) + \sigma^2(\varepsilon_1)\sigma^2(\varepsilon_3)} \\ w_3 = \frac{\sigma^2(\varepsilon_1)\sigma^2(\varepsilon_3)}{\sigma^2(\varepsilon_1)\sigma^2(\varepsilon_2) + \sigma^2(\varepsilon_2)\sigma^2(\varepsilon_3) + \sigma^2(\varepsilon_1)\sigma^2(\varepsilon_3)} \end{cases} \quad (8)$$

where $\sigma^2(\varepsilon_k)$ is the error variance of P_k derived from Equation (4). Note that P_k in Equation (7) can be any precipitation estimate with the error variance derived by TC and is not necessarily the same as the triplet input to TC.

The flowchart of the TCM approach is shown in Figure 2. The SPEs to be merged include IMERG-E, PDIR, and CMORPH in this study. The SM2RAIN-ASCAT and ERA5 products and the SPE constitute the TC triplet. They are input into Equation (4) to derive the error variance of the SPEs (the error variances of the SM2RAIN-ASCAT and ERA5 are derived but not used). Next, the error variances of the SPEs are input into Equation (8) to derive the weights of the SPEs. Finally, the weights are used to generate the multi-SPE merged product via Equation (7).

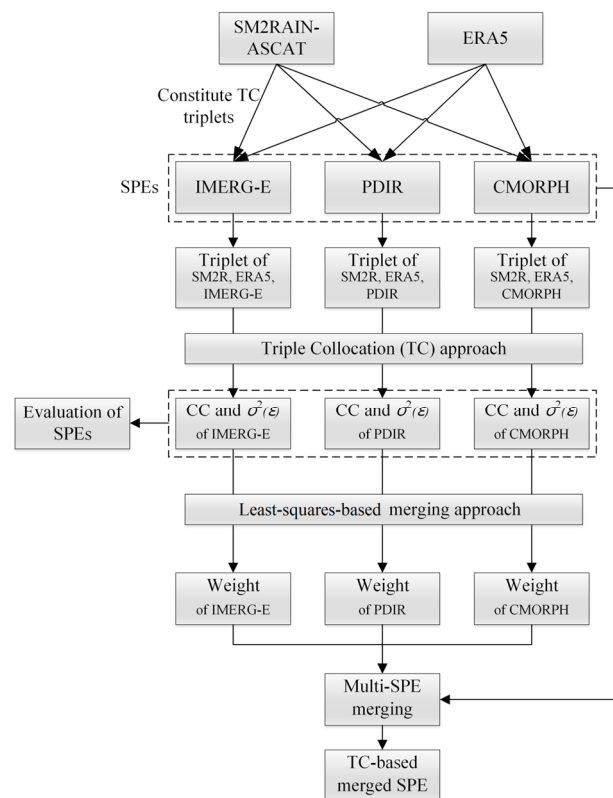


Figure 2. Procedure of the TC-based merging approach.

We compare the TCM approach with the arithmetic mean (AM) approach described by Equation (9), which can be regarded as the equal-weight version of Equation (7):

$$P_{AM} = (P_1 + P_2 + \dots + P_k + \dots + P_n) / n \quad (9)$$

3.3. Assessment Metrics

Four assessment metrics [52] are used to evaluate the performance of the TC-based merged SPEs and the TCM approach in the TP using the gauge data as the benchmark. The performance of the original SPEs is compared with the TCM. The assessment metrics

include the CC to quantify the correlation of the SPEs with the gauge observations, the root mean square error (RMSE) to quantify the overall error of the SPEs, the Nash–Sutcliffe efficiency coefficient (NSE) to quantify the consistency of the SPEs with the observations, and the relative bias (RB) to quantify the relative systematic bias of the SPEs. The equations of the assessment metrics are listed in Table 1. Since the SPEs have a raster format and the gauge observations are point data, the SPE data are interpolated to the location of the gauge stations using a bilinear approach.

Table 1. Equations of assessment metrics.

Metric	Equation *	Perfect Score
Correlation coefficient (CC)	$CC = \frac{\Sigma(P-\bar{P})(O-\bar{O})}{\sqrt{\Sigma(P-\bar{P})^2 \cdot \Sigma(O-\bar{O})^2}}$	1
Root mean square error (RMSE)	$RMSE = \sqrt{\frac{\Sigma(P-O)^2}{n}}$	0
Nash–Sutcliffe efficiency coefficient (NSE)	$NSE = 1 - \frac{\Sigma(P-O)^2}{\Sigma(O-\bar{O})^2}$	1
Relative bias (RB)	$RB = \left(\frac{\bar{P}}{\bar{O}} - 1\right) \times 100\%$	0

* P and O denote the estimations to be assessed and the benchmark data, and \bar{P} and \bar{O} are their mean values, respectively.

Since the CCs of the SPEs based on gauge observations (i.e., the traditional assessment approach) are calculated the same way as those for the TC assessment approach, the gauge-based CC (CC_{trad}) is used as a reference to validate the performance of the TC-derived CC (CC_{TC}).

Note that before assessing the SPE data using the traditional and TC approaches and performing TC-based merging with other SPEs, the SPE data are needed to be converted to the same spatial resolution. Considering that this study focus on the TP with a large spatial scale, and the influence of spatial resolution of SPEs is not the major concern of this study, we converted the three SPEs to the spatial resolution of CMORPH and ERA5 (0.25°) instead of the finest resolution of PDIR (0.04°). The IMERG-E, PDIR, and SM2RAIN data were converted by spatial-averaging the data from their original resolution to 0.25° grid cells.

4. Results

4.1. Validation of the TC Assessment Approach

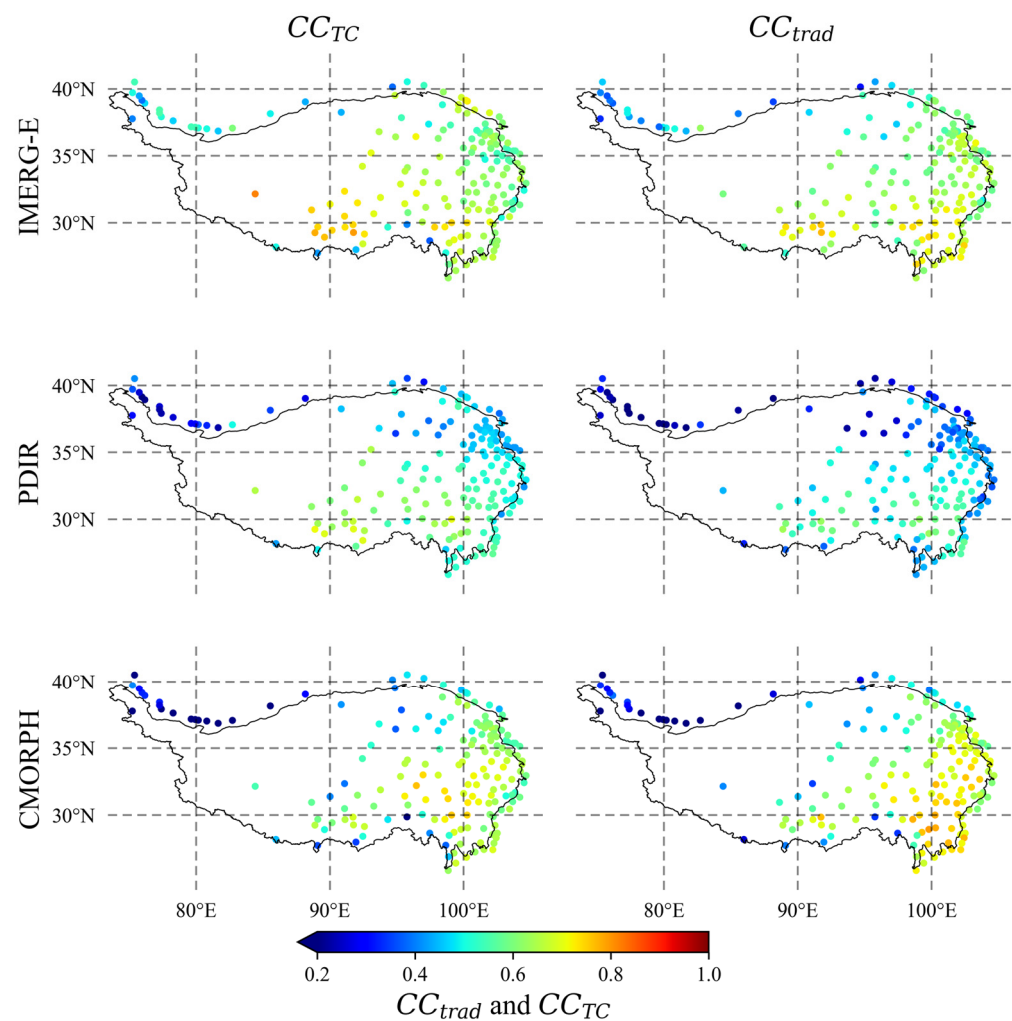
The performance and suitability of the TC assessment approach is validated before performing the TCM for the SPEs in the TP. The CCs of the SPEs based on the traditional and TC approaches are calculated at daily and monthly scales from 2007 to 2018. The mean values of the CC_{TC} and CC_{trad} and the CC between the CC_{TC} and CC_{trad} at the gauge stations are listed in Table 2. The mean CCs derived from the TC approach and the traditional approach are similar. The CCs derived from the traditional and TC approaches show that IMERG-E has the highest accuracy, followed closely by CMORPH and PDIR. Their mean CC_{TC} and CC_{trad} at the daily scale are about 0.6, slightly below 0.6, and below 0.5, respectively. Both assessment approaches show that the accuracy of the three SPEs is higher at the monthly scale than at the daily scale, with mean CC_{TC} and CC_{trad} values of about 0.8. The CC_{TC} also has high consistency with CC_{trad} ; they range from nearly 0.7 to over 0.9, indicating that the TC approach can accurately depict the spatial pattern of the SPEs.

Figures 3 and 4 show the maps of the CC_{TC} and CC_{trad} at the gauge stations for the three SPEs in the TP at daily and monthly scales, respectively. The TC approach exhibits a similar spatial accuracy pattern as the traditional approach for the three SPEs. For instance, both the CC_{TC} and CC_{trad} indicate that the IMERG-E has higher accuracy in the southern and southeastern TP and lower accuracy at the northwest boundary. The PDIR has a similar accuracy pattern as the IMERG-E, but its accuracy is lower. The CC_{TC} and CC_{trad} for the CMORPH show that the areas with the highest accuracy are located in the southeastern TP.

Table 2. CCs of the SPEs derived from the TC and traditional approaches.

Time Scale	Metrics	IMERG-E	PDIR	CMORPH
Daily	Mean value of CC_{TC}	0.612	0.499	0.555
	Mean value of CC_{trad}	0.609	0.429	0.586
	CC between CC_{TC} and CC_{trad}	0.677	0.873	0.938
Monthly	Mean value of CC_{TC}	0.852	0.779	0.807
	Mean value of CC_{trad}	0.823	0.719	0.790
	CC between CC_{TC} and CC_{trad}	0.738	0.812	0.955

Figures 5 and 6 show the accuracy ranking of the SPEs based on the CC_{TC} and CC_{trad} at the daily and monthly scales, respectively. The rank values of 1, 2, and 3 in the figures indicate that the CC value of the SPE is the 1st, 2nd, and 3rd highest among the three SPEs, respectively. The accuracy ranking shows a similar spatial pattern for the TC and traditional approaches. Both the CC_{TC} and CC_{trad} show that the IMERG-E has the highest accuracy in the central, western, and northeastern TP and ranks second in most of the remaining areas. The CMORPH shows the highest accuracy in the eastern TP but performs worse in the western and northwestern areas. The PDIR exhibits the lowest accuracy in most areas but ranks second and first in parts of the western and northwestern TP.

**Figure 3.** Maps of the CCs at the gauge stations for three SPEs at the daily scale derived from the TC and traditional approaches.

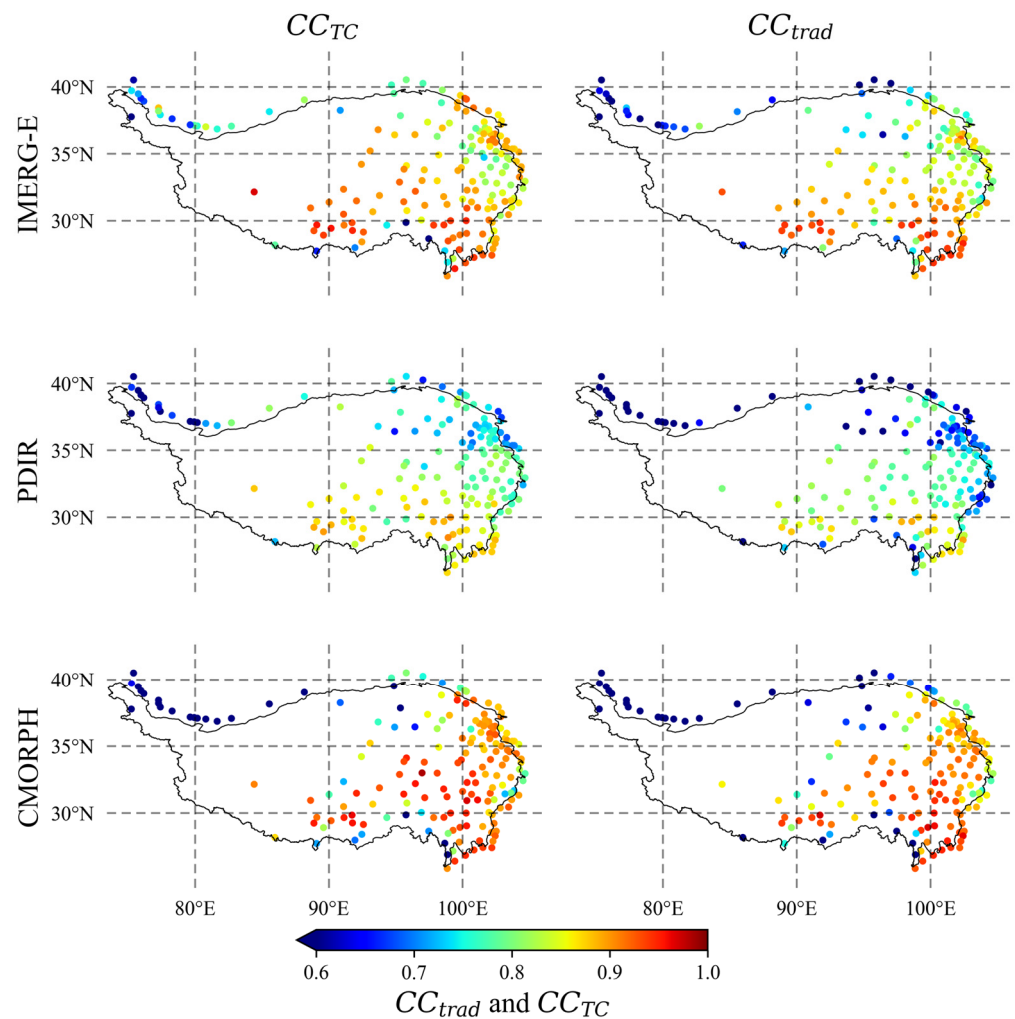


Figure 4. Maps of the CCs at the gauge stations for three SPEs at the monthly scale derived from the TC and traditional approaches.

Overall, the results above show that the TC approach has a reliable performance in assessing the accuracy of SPEs in the TP at daily and monthly scales. It accurately depicts the magnitude and spatial pattern of the CCs of the SPEs and the accuracy ranking of the SPEs in the TP. This finding suggests that the TC approach is applicable for assessing the SPEs' accuracy and data fusion of the SPEs in ungauged areas of the TP.

4.2. Performance of the TC Approach

Figure 7 shows the maps of the CCs of the SPEs based on the TC approach at daily and monthly scales from 2007 to 2018. The spatially continuous TC assessment results provide more information on the SPEs' accuracy than sparse and unevenly distributed point data of the traditional approach. For instance, the IMERG-E shows higher accuracy in the southwestern TP. The CMORPH has much lower accuracy in large areas of the northwestern TP than the PDIR. For the south and east TP, the accuracy of the SPEs is similar. The accuracy patterns of the three SPEs are similar on daily and monthly scales, but the CC values are higher on the monthly scale. These results are not observed in the traditional approach because gauge data are non-existent in most of the western TP. In general, the IMERG-E has the highest accuracy, and the PDIR has the lowest accuracy in the TP, but the accuracy variability is relatively small. The CMORPH exhibits the highest accuracy variability.

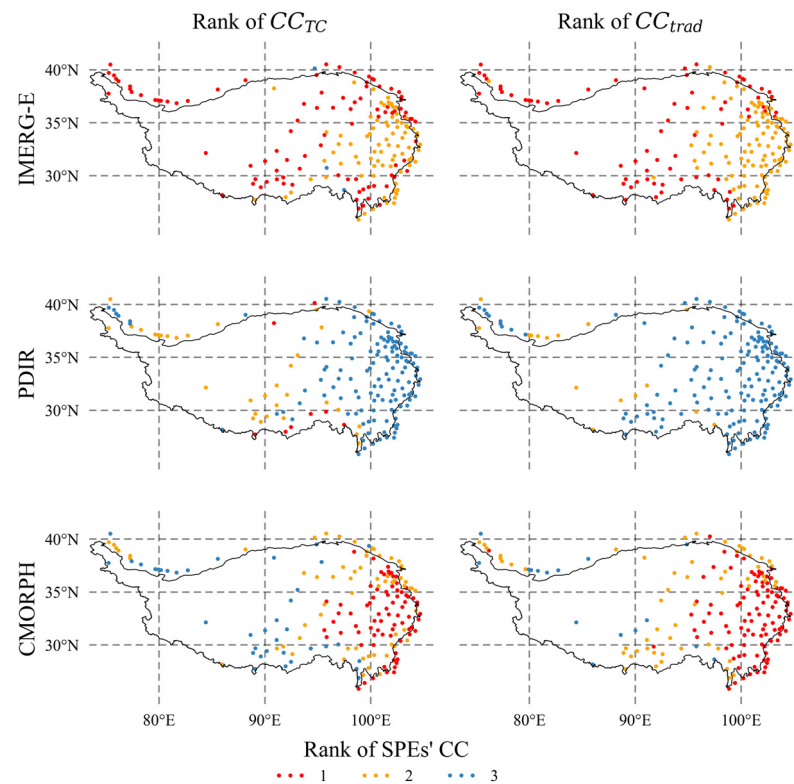


Figure 5. Accuracy ranking of the SPEs based on the CCs derived from the TC and traditional approaches at the daily scale.

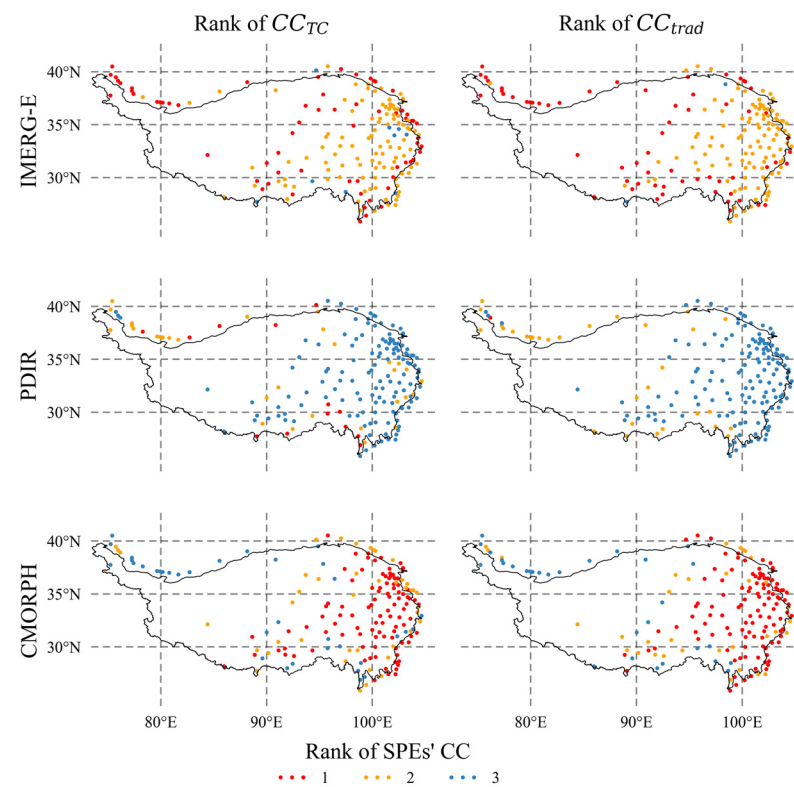


Figure 6. Accuracy rankings of the SPEs based on the CCs derived from the TC and traditional approaches at the monthly scale.

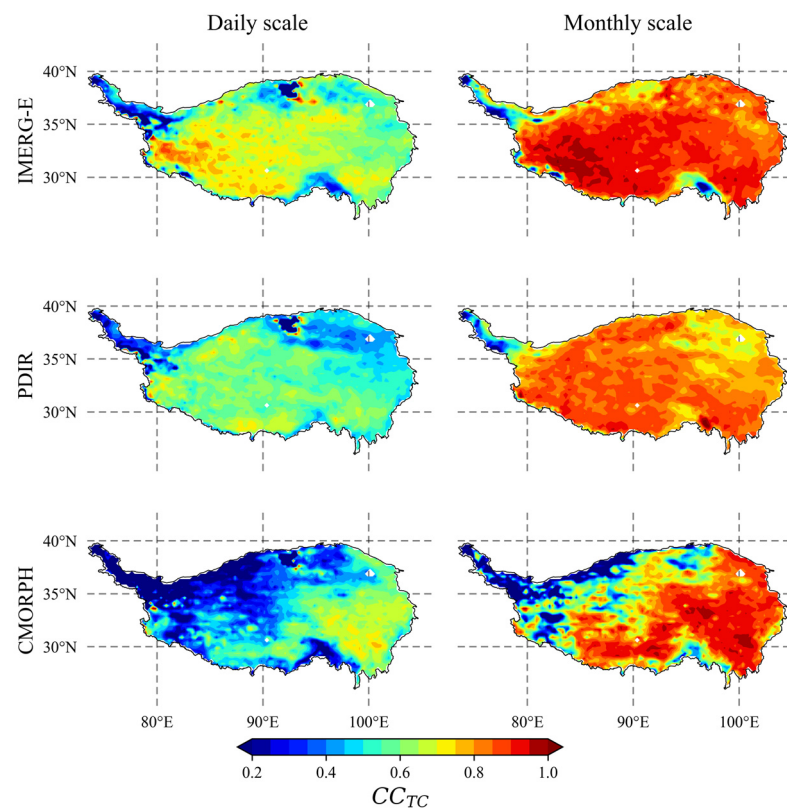


Figure 7. Maps of the CC of SPEs on the TP derived from the TC approach.

4.3. Data Fusion of SPEs Based on the TC Approach

TCM was performed for the SPEs at daily and monthly scales from 2007 to 2018 using the procedure described in Section 3.2. The AM merging approach was used for comparison. The spatial maps of annual mean precipitation from gauge stations, original and merged SPEs are shown in Figure 8. All SPEs show close spatial patterns of precipitation with the gauge observations, with precipitation decreasing from southeast to northwest of TP. Nevertheless, PDIR and CMORPH show an overall overestimation of precipitation, and PDIR shows a smooth spatial pattern, while IMERG-E shows an underestimation in some areas. The TC-merged results generally show a spatial pattern close to gauge data. Note that some severe error in source SPE, like the overestimation over lakes in CMORPH, might be propagated to the merged result. The assessment metrics of the original and merged SPEs based on the gauge data from all stations are listed in Table 3. The boxplots of the assessment metrics are shown in Figures 9 and 10. It is observed that the TCM approach has the highest accuracy, outperforming all original SPEs based on the CCs (0.65 to 0.674 at the daily scale), NSEs (0.38 to 0.44 at the daily scale), RMSEs (3.6 mm to 3.2 mm at the daily scale), and RBs (close to zero). On the monthly scale, the TCM performs better than the original SPEs. The RMSE (NSE) is approximately 30 mm (0.7) for the original SPEs and 25.5 mm (0.8) for the TCM. Figures 9 and 10 also show that the TCM generally has the highest CCs and NSEs and the smallest RMSE, and the range of the assessment metrics is narrower than that of the other SPEs in most conditions, indicating the better stability of the merged SPE derived from TCM. Nevertheless, TCM shows slightly better metrics to the AM, with CCs and NSEs relatively higher than AM, but the improvement is not very significant.

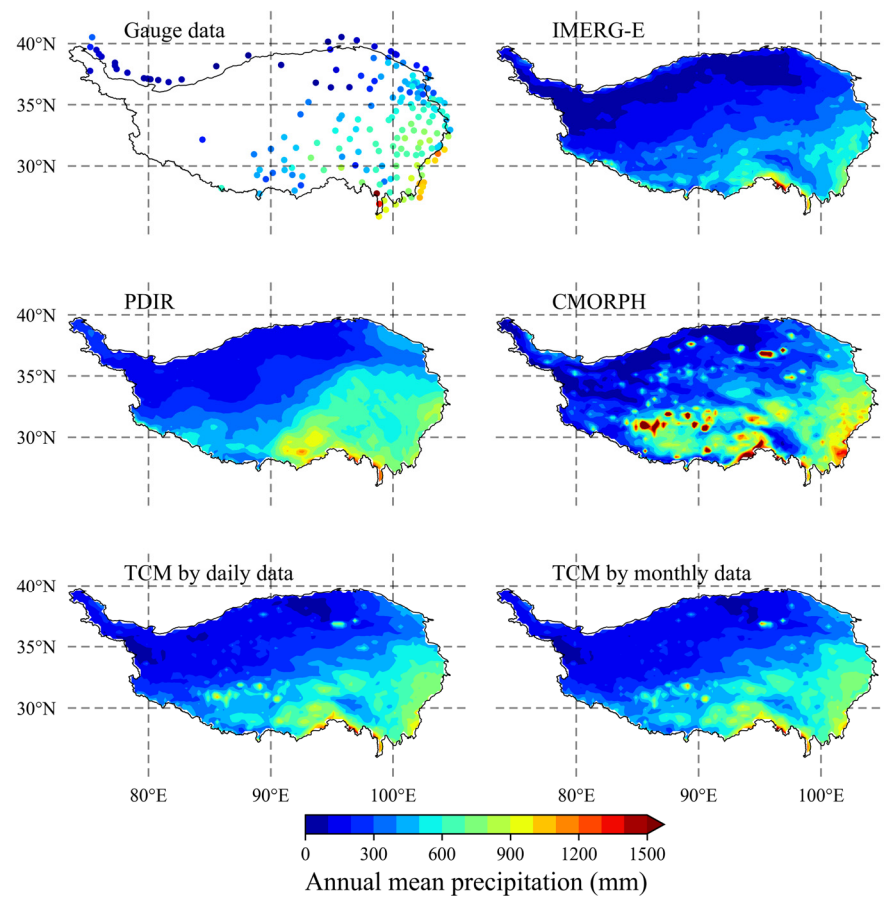


Figure 8. Spatial distribution of annual mean precipitation from gauge stations, SPEs, and TCM results.

Table 3. Assessment metrics of the original and merged SPEs.

SPEs	Daily				Monthly			
	CC	RMSE (mm)	NSE	RB (%)	CC	RMSE (mm)	NSE	RB (%)
IMERG-E	0.640	3.39	0.378	−23.4	0.855	30.77	0.701	−23.4
PDIR	0.470	4.08	0.098	4.9	0.756	38.11	0.541	4.9
CMORPH	0.652	3.61	0.293	12.3	0.864	30.50	0.706	12.3
AM	0.667	3.24	0.432	−2.1	0.884	26.34	0.781	−2.1
TCM	0.674	3.21	0.442	−2.4	0.891	25.50	0.794	−1.4

Figures 11 and 12 show the maps of the assessment metrics of the original and merged SPEs at daily and monthly scales, respectively. Similar to the assessment results shown in Figures 3 and 4, the three original SPEs show different accuracy patterns. The IMERG-E has higher CCs and NSEs at the gauge stations in the southern TP, whereas the CMORPH shows higher CCs and NSEs in the southeastern TP. The TCM-derived SPE incorporates the different regional advantages of the SPEs since it shows high CC and NSE values in the southern and southeastern TP, where the IMERG-E and CMORPH have higher values, respectively. Although the improvement to AM results was not significant, the results also indicate that TCM can perform reasonable and reliable data fusion of the SPEs, improving the performance of the SPEs compared with traditional methods without requiring gauge observations. Therefore, the TCM is reasonable and applicable to sparsely gauged and ungauged areas, such as the TP.

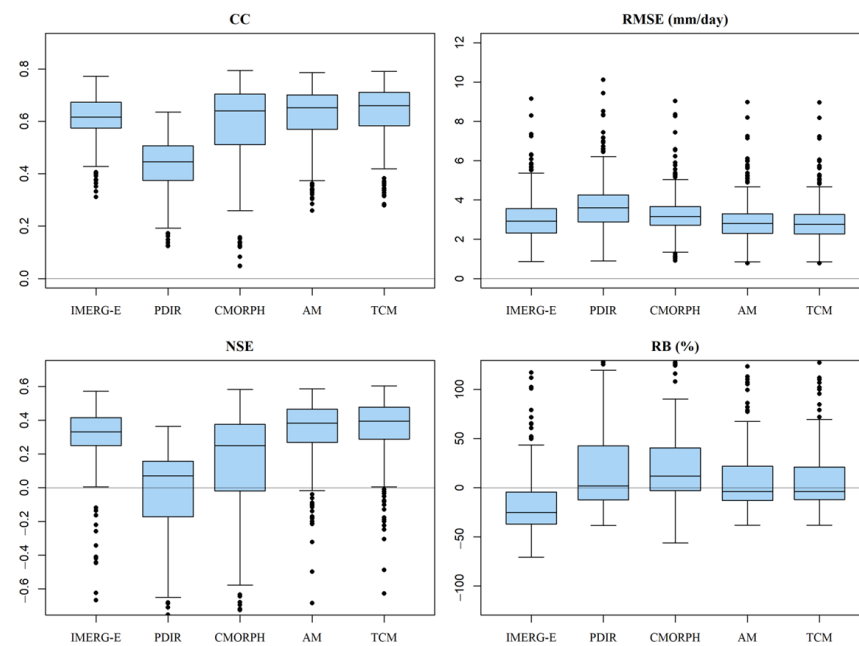


Figure 9. Boxplots of the assessment metrics of the original and merged SPEs at the daily scale for all gauge stations in the TP. Note: The upper and lower edges of the box denote the 75% and 25% quantiles, respectively, the line in the box denotes the median, the horizontal lines outside the box denote the maximum and minimum, and the points denote the outliers.

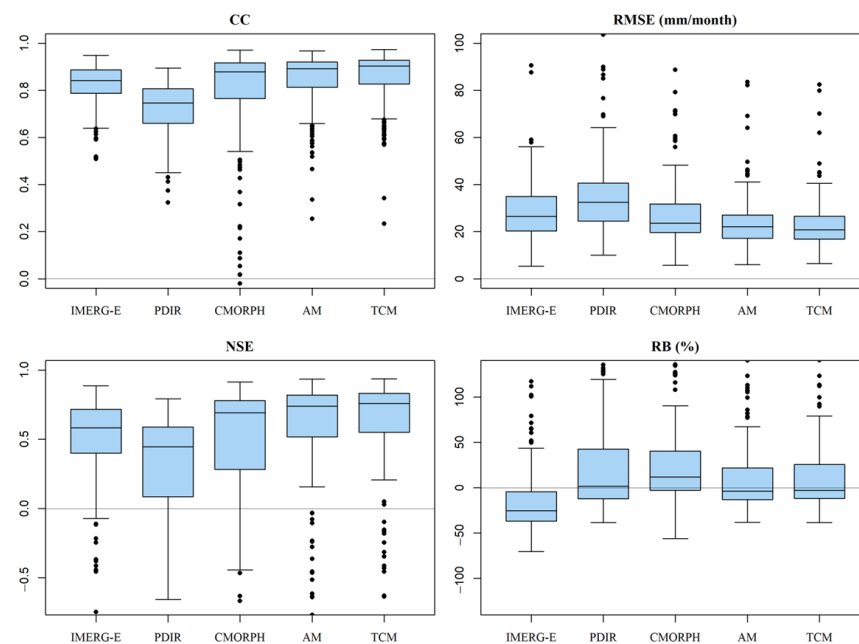


Figure 10. Boxplots of the assessment metrics of the original and merged SPEs at the monthly scale for all gauge stations in the TP.

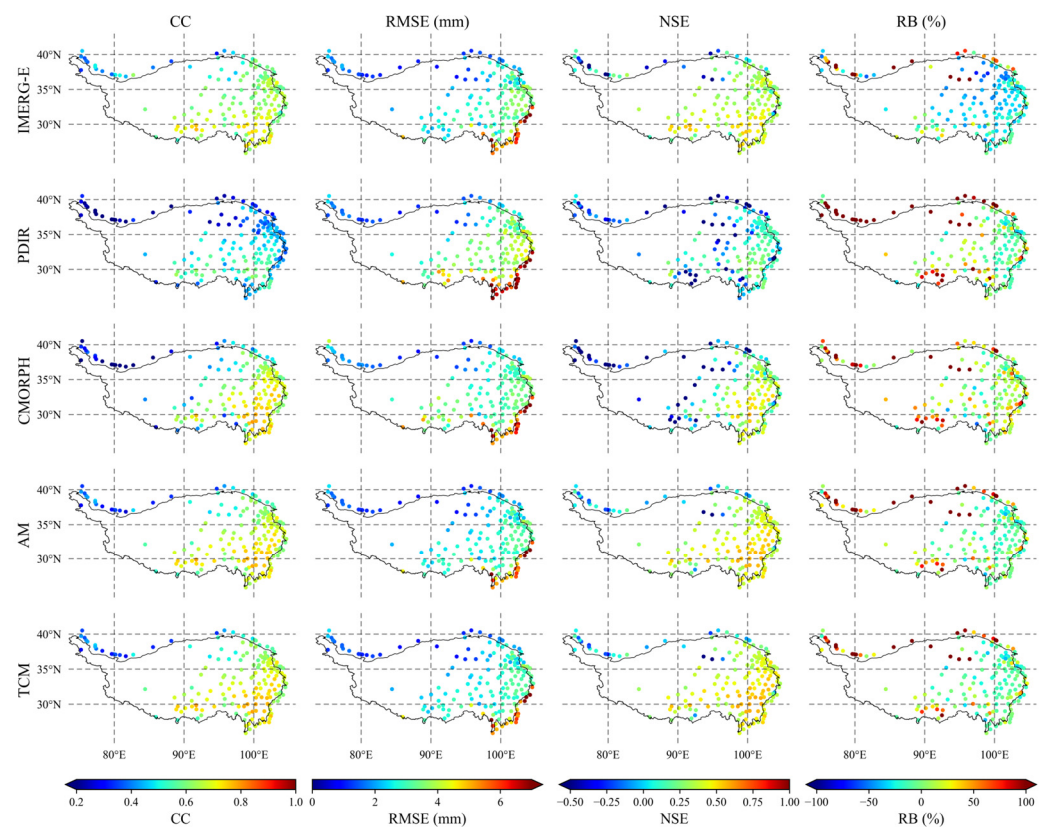


Figure 11. Maps of assessment metrics of the original and merged SPEs at the daily scale.

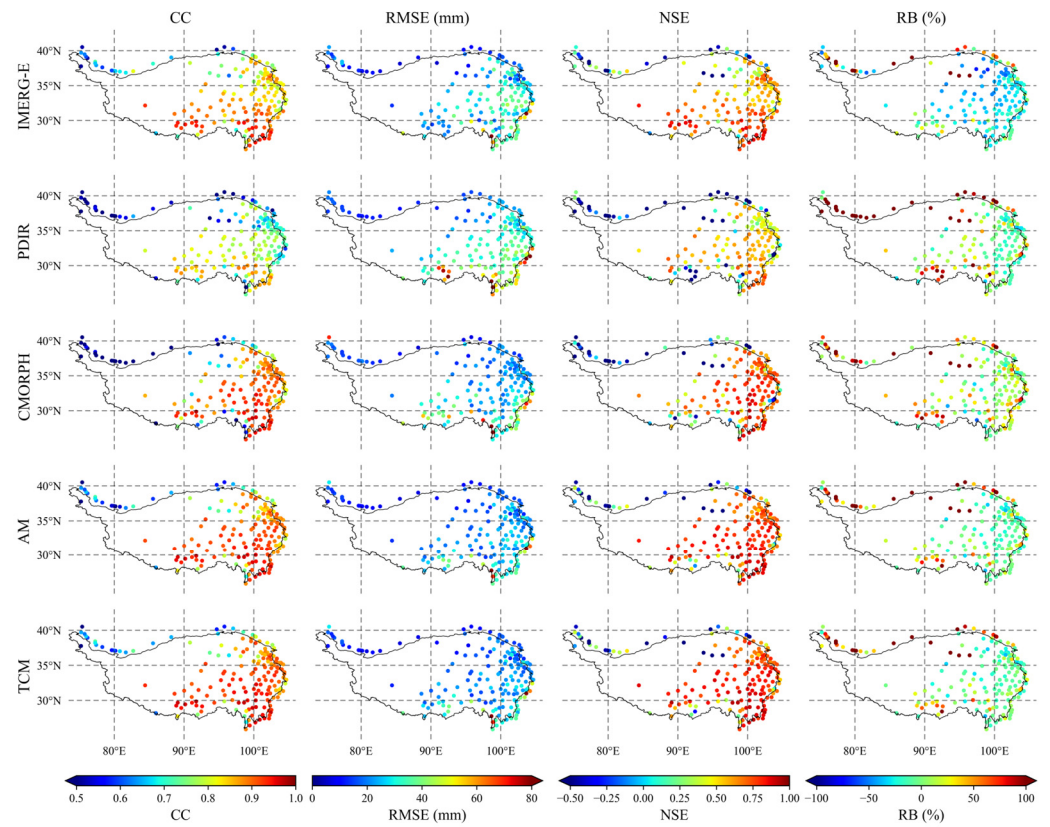


Figure 12. Maps of assessment metrics of the original and merged SPEs at the monthly scale.

5. Discussion

Several studies have assessed SPEs in the TP. Tong et al. [7] evaluated the accuracy of four SPEs for driving hydrological models in the TP based on local gauge data. It was found that the CMORPH and the TMPA 3B42 products performed better over TP. Wei et al. [53] and Lu et al. [54] also assessed several SPEs in the TP, including the IMERG and CMORPH products. Lei et al. [55] performed similar studies but only in the eastern TP, with relatively denser gauge stations. Although the SPE version was different in these studies, the accuracy patterns of the SPEs, including the CMORPH and IMERG products, were similar for traditional and TC approaches, i.e., higher accuracy of the IMERG in the southern TP, whereas the CMORPH was more accurate in the southeastern TP. Some studies analyzed the influence of topography and climate on SPEs' accuracy, and found that poorer accuracy of SPEs was mainly distributed in areas with arid climate and complicated terrain [32,55]. The TC-based assessment results also commonly show poorer CC of SPEs over the arid northwest and northeast (Qaidam basin) regions. Nevertheless, these former studies used the traditional approach based on gauge data; therefore, the accuracy of the SPEs could not be determined in ungauged areas, such as the northwestern TP. Spatial interpolation of gauge data over ungauged areas might be a solution, but reliability cannot be ensured, as Li et al. [32] observed lower accuracy of gauge-interpolated data. Therefore, we used the TC approach, which does not require benchmark data, to obtain data in ungauged areas, which is not possible with the traditional approach. Some studies, such as that by Li et al. [32], also used the TC approach to assess SPEs in mainland China, including the TP. Although they used different inputs to create the TC triplet (gauge-interpolated data instead of SM2RAIN), their results showed similar accuracy patterns in the TP to our study, indicating the stability of the TC approach. Nevertheless, most of these studies used daily data for the assessment. In contrast, we evaluated the SPEs at daily and monthly scales to demonstrate the applicability of the TC approach.

Data fusion of SPEs and other precipitation products is typically performed to obtain relatively higher accuracy of precipitation estimates, especially in areas with sparse gauge data, such as the TP [15]. For instance, Wang et al. [56] proposed a data fusion approach for precipitation data based on Bayesian model averaging (BMA). Based on this, Ma et al. [4] proposed the dynamic BMA to merge SPEs, considering the temporal variation of the SPEs' accuracy. Baez-Villanueva et al. [57] proposed a data fusion approach for precipitation data based on random forest. However, these studies relied on gauge observations to determine the error or accuracy characteristic of data inputs as prior information for reasonable data fusion. Therefore, this method might be limited for ungauged areas unless the data fusion parameters (e.g., average weights) can be interpolated from surrounding gauge stations [4]. The TC approach provides a new solution for deriving a priori accuracy information on the SPEs in ungauged areas. Our study demonstrates the ability of the TC approach to retrieve the spatial accuracy pattern and accuracy ranking of the three SPEs; thus, the TC approach has great potential for providing a priori accuracy information for data fusion. TC-based data fusion has been validated by Lyu et al. [42], Dong et al. [41], and Chen et al. [13], who found that the TCM results showed comparable performance to gauge-based data fusion approaches, such as BMA. In these studies, the precipitation datasets comprising the triplets input to the TC assessment were used as input to data fusion. Since the SM2RAIN data do not include near-real-time precipitation monitoring and historical records before 2007, the temporal range of SPEs for data fusion is limited, especially for long-term or near-real-time products. Thus, this study used only the ERA5 and SM2RAIN for accuracy assessment and determination of the merging weight of the three SPEs separately via the TC approach to perform TC-based data fusion for multiple SPEs. Our results also show performance and stability of the merged SPEs as higher than the original SPEs in the TP, indicating the suitability of the TC approach for merging an arbitrary number (over 2) of SPEs since their accuracy characteristic can be individually derived by TC.

Moreover, it is worth to note that, compared with the arithmetic mean approach, the TC-based merging results show better values of assessment metrics, but the discrepancies

are not very significant. Yilmaz et al. [40] also found that the TC merging did not show significant improvement to AM results, and pointed out that similar weights of the merging source is an important reason. Figure A1 in the Appendix A shows the spatial patterns of the TC-based weights of the tree SPEs based on daily and monthly precipitation, which are similar to the TC assessment results shown in Figure 7. The areas with large discrepancy in TC-based weight generally are distributed in the west and north of TP where no gauge stations are available. For the east and south TP where gauge data as validation benchmarks are dense, the weights of the SPEs are similar. These might be the causes of the insignificant improvement of TCM to AM since AM is substantially an equal-weight merging approach. Above all, the TCM can still be regarded as a reliable SPE fusion approach when gauge data are unavailable.

Additionally, in practical conditions, spatial resolution would also be an important factor to be considered in selection of SPEs for merging. In this study, considering that the TP as the study area has a large spatial scale, and downscaling the SPE data from coarse to finer resolution usually has larger uncertainty than upscaling, this study converted all SPEs to the coarsest 0.25° resolution. Relative studies over the mountainous area have also pointed out that upscaling the fine resolution SPE (0.1° and 0.05°) to coarse resolution (0.25°) has little influence on the assessed accuracy [55,58]. Therefore, we suggest that, for the considered large spatial scale in this study, the discrepancy in spatial resolution of SPEs has no substantial influence on our results. Nevertheless, for the applications over the small basins, high spatial resolution might be a requirement when selecting SPEs and performing a TC approach. Considering that reanalysis by ERA5 and SM2RAIN as necessary TC triplets might not be easily substituted by finer products, spatial downscaling for these data to fit the resolution of fine SPEs might be a solution. The spatial downscaling of SPEs is out of the scope of this study and, thus, is not discussed.

6. Conclusions

This study conducted an assessment and data fusion of SPE products in the TP, an area with important significance in hydrology and global climate but sparse gauge observations. The TC approach was used because it provides the accuracy and error of the SPEs without requiring gauge data. Three widely used SPEs were investigated: IMERG-E, PDIR, and CMORPH.

The validation based on the traditional assessment approach showed that the TC approach provided similar performance for the accuracy assessment of the SPEs. It provided accurate magnitudes and spatial patterns of the SPEs' CCs. The CC of the TC and traditional assessment results were 0.7 and 0.95 at most gauge stations. Moreover, the TC approach also provided an accurate accuracy ranking of the SPEs in the TP.

The assessment results of the TC approach showed that the IMERG-E, generally, had the highest accuracy, the PDIR had the lowest accuracy, and the CMORPH exhibited high accuracy variability in the TP. The TC approach also provided more information on the accuracy pattern of the SPEs in ungauged areas of the TP than the point-based traditional method, depicting the high accuracy of the IMERG-F in the southwestern TP. These findings cannot be obtained by the gauge-based traditional approach because gauge data are unavailable in these areas.

The data fusion results showed that the TCM approach provided better performance than the original SPEs because it incorporates the regional advantages of the individual SPEs. The CCs (NSEs) were 0.65 (0.38) for the original SPEs and 0.674 (0.44) for the TCM approach at the daily scale, and the RBs were close to zero for the TCM approach, demonstrating the reasonability and reliability of the TC approach for merging multiple SPEs in ungauged areas. Nevertheless, the improvement of TCM approach to the AM-based fusion method that uses equal-weight averaging is not significant, and the similar TC-based weights of SPEs over the gauged product for validation might be the major reason.

Our results indicate the TC approach is reasonable and applicable for assessing the SPE accuracy and performing data fusion of SPEs in the TP, an area with sparse and uneven

gauge observations. Since the TC approach does not require gauge observations, the TC-based assessment and data fusion can be used in other areas without gauge data.

Author Contributions: Software, X.W.; Validation, X.W.; Formal analysis, X.W.; Resources, J.Z.; Data curation, J.Z.; Writing—original draft, X.W.; Writing—review & editing, C.L.; Supervision, C.L.; Funding acquisition, C.L. All authors have read and agreed to the published version of the manuscript.

Funding: The research acquired financial or data support by the National Key R&D Program of China (number 2021YFC3001000), the Natural Science Foundation of Guangdong Province (number 2023B1515020087), and the Science and Technology Program of Guangzhou (number 202102020216).

Data Availability Statement: Not applicable.

Conflicts of Interest: The authors declare no conflict of interest.

Appendix A

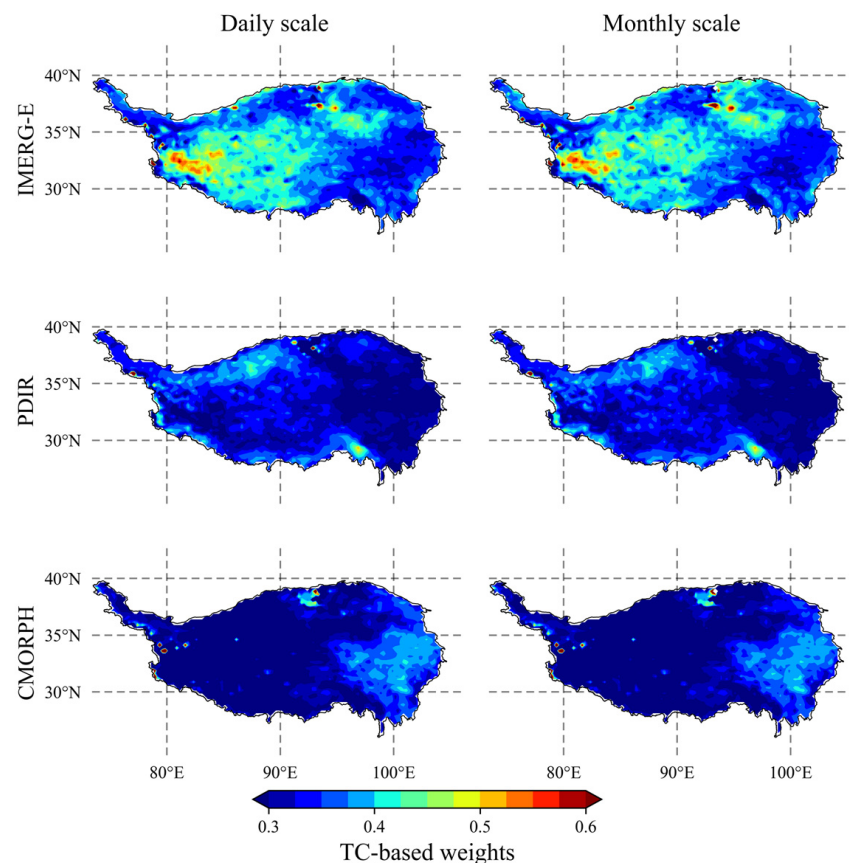


Figure A1. Maps of the TC-based weights of SPEs on the TP for TC-based merging approach.

References

1. Li, X.; Long, D.; Scanlon, B.R.; Mann, M.E.; Li, X.; Tian, F.; Sun, Z.; Wang, G. Climate change threatens terrestrial water storage over the Tibetan Plateau. *Nat. Clim. Chang.* **2022**, *12*, 801. [[CrossRef](#)]
2. Tang, G.; Clark, M.P.; Papalexiou, S.M.; Ma, Z.; Hong, Y. Have satellite precipitation products improved over last two decades? A comprehensive comparison of GPM IMERG with nine satellite and reanalysis datasets. *Remote Sens. Environ.* **2020**, *240*, 111697. [[CrossRef](#)]
3. Bai, X.; Wu, X.; Wang, P. Blending long-term satellite-based precipitation data with gauge observations for drought monitoring: Considering effects of different gauge densities. *J. Hydrol.* **2019**, *577*, 124007. [[CrossRef](#)]
4. Ma, Y.; Hong, Y.; Chen, Y.; Yang, Y.; Tang, G.; Yao, Y.; Long, D.; Li, C.; Han, Z.; Liu, R. Performance of Optimally Merged Multisatellite Precipitation Products Using the Dynamic Bayesian Model Averaging Scheme over the Tibetan Plateau. *J. Geophys. Res. Atmos.* **2018**, *123*, 814–834. [[CrossRef](#)]

5. Wang, Z.; Zhong, R.; Lai, C. Evaluation and hydrologic validation of TMPA satellite precipitation product downstream of the Pearl River Basin, China. *Hydrol. Process.* **2017**, *31*, 4169–4182. [[CrossRef](#)]
6. Ma, Y.; Zhang, Y.; Yang, D.; Farhan, S.B. Precipitation bias variability versus various gauges under different climatic conditions over the Third Pole Environment (TPE) region. *Int. J. Climatol.* **2015**, *35*, 1201–1211. [[CrossRef](#)]
7. Tong, K.; Su, F.; Yang, D.; Hao, Z. Evaluation of satellite precipitation retrievals and their potential utilities in hydrologic modeling over the Tibetan Plateau. *J. Hydrol.* **2014**, *519*, 423–437. [[CrossRef](#)]
8. Hsu, K.; Gao, X.; Sorooshian, S.; Gupta, H.V. Precipitation Estimation from Remotely Sensed Information Using Artificial Neural Networks. *J. Appl. Meteorol.* **1997**, *36*, 1176–1190. [[CrossRef](#)]
9. Joyce, R.J.; Janowiak, J.E.; Arkin, P.A.; Xie, P. CMORPH: A Method that Produces Global Precipitation Estimates from Passive Microwave and Infrared Data at High Spatial and Temporal Resolution. *J. Hydrometeorol.* **2004**, *5*, 487–503. [[CrossRef](#)]
10. Huffman, G.J.; Bolvin, D.T.; Nelkin, E.J.; Wolff, D.B.; Adler, R.F.; Gu, G.; Hong, Y.; Bowman, K.P.; Stocker, E.F. The TRMM Multisatellite Precipitation Analysis (TMPA): Quasi-Global, Multiyear, Combined-Sensor Precipitation Estimates at Fine Scales. *J. Hydrometeorol.* **2007**, *8*, 38–55. [[CrossRef](#)]
11. Huffman, G.J.; Bolvin, D.T.; Braithwaite, D.; Hsu, K.; Joyce, R.; Kidd, C.; Nelkin, E.J.; Sorooshian, S.; Stocker, E.F.; Tan, J.; et al. *Integrated Multi-Satellite Retrievals for the Global Precipitation Measurement (GPM) Mission (IMERG)*; Levizzani, V., Kidd, C., Kirschbaum, D.B., Kummerow, C.D., Nakamura, K., Turk, F.J., Eds.; Satellite Precipitation Measurement; Springer International Publishing: Cham, Switzerland, 2020; Volume 1, pp. 343–353.
12. Hou, A.Y.; Kakar, R.K.; Neeck, S.; Azarbarzin, A.A.; Kummerow, C.D.; Kojima, M.; Oki, R.; Nakamura, K.; Iguchi, T. The Global Precipitation Measurement Mission. *Bull. Am. Meteorol. Soc.* **2014**, *95*, 701–722. [[CrossRef](#)]
13. Chen, C.; He, M.; Chen, Q.; Zhang, J.; Li, Z.; Wang, Z.; Duan, Z. Triple collocation-based error estimation and data fusion of global gridded precipitation products over the Yangtze River basin. *J. Hydrol.* **2022**, *605*, 127307. [[CrossRef](#)]
14. Xie, P.; Arkin, P.A. Global Precipitation: A 17-Year Monthly Analysis Based on Gauge Observations, Satellite Estimates, and Numerical Model Outputs. *Bull. Am. Meteorol. Soc.* **1997**, *78*, 2539–2558. [[CrossRef](#)]
15. Ma, Y.; Sun, X.; Chen, H.; Hong, Y.; Zhang, Y. A two-stage blending approach for merging multiple satellite precipitation estimates and rain gauge observations: An experiment in the northeastern Tibetan Plateau. *Hydrol. Earth Syst. Sci.* **2021**, *25*, 359–374. [[CrossRef](#)]
16. Wu, H.; Yang, Q.; Liu, J.; Wang, G. A spatiotemporal deep fusion model for merging satellite and gauge precipitation in China. *J. Hydrol.* **2020**, *584*, 124664. [[CrossRef](#)]
17. Chen, J.; Wang, Z.; Wu, X.; Lai, C.; Chen, X. Evaluation of TMPA 3B42-V7 Product on Extreme Precipitation Estimates. *Remote Sens.* **2021**, *13*, 209. [[CrossRef](#)]
18. Bai, X.; Shen, W.; Wu, X.; Wang, P. Applicability of long-term satellite-based precipitation products for drought indices considering global warming. *J. Environ. Manag.* **2020**, *255*, 109846. [[CrossRef](#)]
19. Lai, C.; Zhong, R.; Wang, Z.; Wu, X.; Chen, X.; Wang, P.; Lian, Y. Monitoring hydrological drought using long-term satellite-based precipitation data. *Sci. Total Environ.* **2019**, *649*, 1198–1208. [[CrossRef](#)] [[PubMed](#)]
20. Bai, P.; Liu, X. Evaluation of Five Satellite-Based Precipitation Products in Two Gauge-Scarce Basins on the Tibetan Plateau. *Remote Sens.* **2018**, *10*, 1316. [[CrossRef](#)]
21. Wang, Z.; Zhong, R.; Lai, C.; Chen, J. Evaluation of the GPM IMERG satellite-based precipitation products and the hydrological utility. *Atmos. Res.* **2017**, *196*, 151–163. [[CrossRef](#)]
22. Ma, Y.; Tang, G.; Long, D.Y.B.; Zhong, L.W.W.; Hong, Y. Similarity and Error Intercomparison of the GPM and Its Predecessor-TRMM Multisatellite Precipitation Analysis Using the Best Available Hourly Gauge Network over the Tibetan Plateau. *Remote Sens.* **2016**, *8*, 569. [[CrossRef](#)]
23. Tang, G.; Ma, Y.; Long, D.; Zhong, L.; Hong, Y. Evaluation of GPM Day-1 IMERG and TMPA Version-7 legacy products over Mainland China at multiple spatiotemporal scales. *J. Hydrol.* **2016**, *533*, 152–167. [[CrossRef](#)]
24. Yong, B.; Ren, L.; Hong, Y.; Wang, J.; Gourley, J.J.; Jiang, S.; Chen, X.; Wang, W. Hydrologic evaluation of Multisatellite Precipitation Analysis standard precipitation products in basins beyond its inclined latitude band: A case study in Laohahe basin, China. *Water Resour. Res.* **2010**, *46*, W07542. [[CrossRef](#)]
25. Zhang, L.; Li, X.; Zheng, D.; Zhang, K.; Ma, Q.; Zhao, Y.; Ge, Y. Merging multiple satellite-based precipitation products and gauge observations using a novel double machine learning approach. *J. Hydrol.* **2021**, *594*, 125969. [[CrossRef](#)]
26. Chen, S.; Xiong, L.; Ma, Q.; Kim, J.; Chen, J.; Xu, C. Improving daily spatial precipitation estimates by merging gauge observation with multiple satellite-based precipitation products based on the geographically weighted ridge regression method. *J. Hydrol.* **2020**, *589*, 125156. [[CrossRef](#)]
27. McColl, K.A.; Vogelzang, J.; Konings, A.G.; Entekhabi, D.; Piles, M.; Stoffelen, A. Extended triple collocation: Estimating errors and correlation coefficients with respect to an unknown target. *Geophys. Res. Lett.* **2014**, *41*, 6229–6236. [[CrossRef](#)]
28. Stoffelen, A. Toward the true near-surface wind speed: Error modeling and calibration using triple collocation. *J. Geophys. Res. Ocean.* **1998**, *103*, 7755–7766. [[CrossRef](#)]
29. Chen, F.; Crow, W.T.; Bindlish, R.; Colliander, A.; Burgin, M.S.; Asanuma, J.; Aida, K. Global-scale evaluation of SMAP, SMOS and ASCAT soil moisture products using triple collocation. *Remote Sens. Environ.* **2018**, *214*, 1–13. [[CrossRef](#)]
30. Li, H.; Chai, L.; Crow, W.; Dong, J.; Liu, S.; Zhao, S. The reliability of categorical triple collocation for evaluating soil freeze/thaw datasets. *Remote Sens. Environ.* **2022**, *281*, 113240. [[CrossRef](#)]

31. Yin, G.; Park, J. The use of triple collocation approach to merge satellite- and model-based terrestrial water storage for flood potential analysis. *J. Hydrol.* **2021**, *603*, 127197. [[CrossRef](#)]
32. Li, C.; Tang, G.; Hong, Y. Cross-evaluation of ground-based, multi-satellite and reanalysis precipitation products: Applicability of the Triple Collocation method across Mainland China. *J. Hydrol.* **2018**, *562*, 71–83. [[CrossRef](#)]
33. Alemohammad, S.H.; McColl, K.A.; Konings, A.G.; Entekhabi, D.; Stoffelen, A. Characterization of precipitation product errors across the United States using multiplicative triple collocation. *Hydrol. Earth Syst. Sci.* **2015**, *19*, 3489–3503. [[CrossRef](#)]
34. Wang, P.; Bai, X.; Wu, X.; Lai, C.; Zhang, Z. Spatially continuous assessment of satellite-based precipitation products using triple collocation approach and discrete gauge observations via geographically weighted regression. *J. Hydrol.* **2022**, *608*, 127640. [[CrossRef](#)]
35. Lu, X.; Tang, G.; Liu, X.; Wang, X.; Liu, Y.; Wei, M. The potential and uncertainty of triple collocation in assessing satellite precipitation products in Central Asia. *Atmos. Res.* **2021**, *252*, 105452. [[CrossRef](#)]
36. Cao, D.; Li, H.; Hou, E.; Song, S.; Lai, C. Assessment and Hydrological Validation of Merged Near-Real-Time Satellite Precipitation Estimates Based on the Gauge-Free Triple Collocation Approach. *Remote Sens.* **2022**, *14*, 3835. [[CrossRef](#)]
37. Massari, C.; Crow, W.; Brocca, L. An assessment of the performance of global rainfall estimates without ground-based observations. *Hydrol. Earth Syst. Sci.* **2017**, *21*, 4347–4361. [[CrossRef](#)]
38. Bai, X.; Wang, P.; He, Y.; Zhang, Z.; Wu, X. Assessing the accuracy and drought utility of long-term satellite-based precipitation estimation products using the triple collocation approach. *J. Hydrol.* **2021**, *603*, 127098. [[CrossRef](#)]
39. Brocca, L.; Filippucci, P.; Hahn, S.; Ciabatta, L.; Massari, C.; Camici, S.; Schüller, L.; Bojkov, B.; Wagner, W. SM2RAIN–ASCAT (2007–2018): Global daily satellite rainfall data from ASCAT soil moisture observations. *Earth Syst. Sci. Data* **2019**, *11*, 1583–1601. [[CrossRef](#)]
40. Yilmaz, M.T.; Crow, W.T.; Anderson, M.C.; Hain, C. An objective methodology for merging satellite-and model-based soil moisture products. *Water Resour. Res.* **2012**, *48*, W11502. [[CrossRef](#)]
41. Dong, J.; Lei, F.; Wei, L. Triple Collocation Based Multi-Source Precipitation Merging. *Front. Water.* **2020**, *2*. [[CrossRef](#)]
42. Lyu, F.; Tang, G.; Behrangi, A.; Wang, T.; Tan, X.; Ma, Z.; Xiong, W. Precipitation Merging Based on the Triple Collocation Method Across Mainland China. *IEEE Trans. Geosci. Remote.* **2021**, *59*, 3161–3176. [[CrossRef](#)]
43. Zheng, J.; Zuo, Z.; Lin, Z.; Xiao, D.; Liang, Q. Linkage of the surface air temperature over Tibetan Plateau and Northeast hemisphere in winter at interannual timescale. *Atmos. Res.* **2022**, *274*, 106229. [[CrossRef](#)]
44. Zhong, R.; Zhao, T.; Chen, X. Evaluating the tradeoff between hydropower benefit and ecological interest under climate change: How will the water-energy-ecosystem nexus evolve in the upper Mekong basin? *Energy* **2021**, *237*, 121518. [[CrossRef](#)]
45. Zhang, G.; Yao, T.; Xie, H.; Yang, K.; Zhu, L.; Shum, C.; Bolch, T.; Yi, S.; Allen, S.; Jiang, L.; et al. Response of Tibetan Plateau lakes to climate change: Trends, patterns, and mechanisms. *Earth-Sci. Rev.* **2020**, *208*, 103269.
46. Yang, K.; Wu, H.; Qin, J.; Lin, C.; Tang, W.; Chen, Y. Recent climate changes over the Tibetan Plateau and their impacts on energy and water cycle: A review. *Global Planet. Change* **2014**, *112*, 79–91.
47. Nguyen, P.; Shearer, E.J.; Ombadi, M.; Gorooh, V.A.; Hsu, K.; Sorooshian, S.; Logan, W.S.; Ralph, M. PERSIANN Dynamic Infrared–Rain Rate Model (PDIR) for High-Resolution, Real-Time Satellite Precipitation Estimation. *Bull. Am. Meteorol. Soc.* **2020**, *101*, E286–E302.
48. Hong, Y.; Hsu, K.; Sorooshian, S.; Gao, X. Precipitation Estimation from Remotely Sensed Imagery Using an Artificial Neural Network Cloud Classification System. *J. Appl. Meteorol.* **2004**, *43*, 1834–1853. [[CrossRef](#)]
49. Hersbach, H.; Bell, B.; Berrisford, P.; Hirahara, S.; Horányi, A.; Muñoz-Sabater, J.; Nicolas, J.; Peubey, C.; Radu, R.; Schepers, D.; et al. The ERA5 global reanalysis. *Q. J. Roy. Meteor. Soc.* **2020**, *146*, 1999–2049. [[CrossRef](#)]
50. Brocca, L.; Moramarco, T.; Melone, F.; Wagner, W. A new method for rainfall estimation through soil moisture observations. *Geophys. Res. Lett.* **2013**, *40*, 853–858. [[CrossRef](#)]
51. Brocca, L.; Ciabatta, L.; Massari, C.; Moramarco, T.; Hahn, S.; Hasenauer, S.; Kidd, R.; Dorigo, W.; Wagner, W.; Levizzani, V. Soil as a natural rain gauge: Estimating global rainfall from satellite soil moisture data. *J. Geophys. Res. Atmos.* **2014**, *119*, 5128–5141. [[CrossRef](#)]
52. Huang, Z.; Zhao, T. Predictive performance of ensemble hydroclimatic forecasts: Verification metrics, diagnostic plots and forecast attributes. *WIREs Water* **2022**, *9*, e1580. [[CrossRef](#)]
53. Wei, G.; Lü, H.T.; Crow, W.; Zhu, Y.; Wang, J.; Su, J. Evaluation of Satellite-Based Precipitation Products from IMERG V04A and V03D, CMORPH and TMPA with Gauged Rainfall in Three Climatologic Zones in China. *Remote Sens.* **2018**, *10*, 30. [[CrossRef](#)]
54. Lu, D.; Yong, B. Evaluation and Hydrological Utility of the Latest GPM IMERG V5 and GSMaP V7 Precipitation Products over the Tibetan Plateau. *Remote Sens.* **2018**, *10*, 2022. [[CrossRef](#)]
55. Lei, H.; Li, H.; Zhao, H.; Ao, T.; Li, X. Comprehensive evaluation of satellite and reanalysis precipitation products over the eastern Tibetan plateau characterized by a high diversity of topographies. *Atmos. Res.* **2021**, *259*, 105661. [[CrossRef](#)]
56. Wang, Q.J.; Schepen, A.; Robertson, D.E. Merging Seasonal Rainfall Forecasts from Multiple Statistical Models through Bayesian Model Averaging. *J. Clim.* **2012**, *25*, 5524–5537. [[CrossRef](#)]

57. Baez-Villanueva, O.M.; Zambrano-Bigiarini, M.; Beck, H.E.; McNamara, I.; Ribbe, L.; Nauditt, A.; Birkel, C.; Verbist, K.; Giraldo-Osorio, J.D.; Xuan Thinh, N. RF-MEP: A novel Random Forest method for merging gridded precipitation products and ground-based measurements. *Remote Sens. Environ.* **2020**, *239*, 111606.
58. Duan, Z.; Liu, J.; Tuo, Y.; Chiogna, G.; Disse, M. Evaluation of eight high spatial resolution gridded precipitation products in Adige Basin (Italy) at multiple temporal and spatial scales. *Sci. Total Environ.* **2016**, *573*, 1536–1553. [[CrossRef](#)] [[PubMed](#)]

Disclaimer/Publisher’s Note: The statements, opinions and data contained in all publications are solely those of the individual author(s) and contributor(s) and not of MDPI and/or the editor(s). MDPI and/or the editor(s) disclaim responsibility for any injury to people or property resulting from any ideas, methods, instructions or products referred to in the content.